J|A|C|S
ARTICLES
Published on Web 12/13/2001

The Effect of Mechanical Interlocking on Crystal Packing: Predictions and Testing

Fabio Biscarini,[†] Massimiliano Cavallini,[†] David A. Leigh,*[,‡] Salvador León,[§] Simon J. Teat,[||] Jenny K. Y. Wong,[‡] and Francesco Zerbetto*[,§]

Contribution from the Consiglio Nazionale delle Ricerche, Istituto di Spettroscopia Molecolare, Via P. Gobetti 101, 40129, Bologna, Italy, Centre for Supramolecular and Macromolecular Chemistry, Department of Chemistry, University of Warwick, Coventry CV4 7AL, U.K., Dipartimento di Chimica "G. Ciamician", Università degli Studi di Bologna, V. F. Selmi 2, I-40126, Bologna, Italy, and CLRC Daresbury Laboratory, Warrington, Cheshire, WA4 4AD, U.K.

Received April 3, 2001. Revised Manuscript Received September 18, 2001

Abstract: The first statistical analyses of the X-ray crystal structures of mechanically interlocked molecular architectures, the first molecular mechanics-based solid-state calculations on such structures and atomic force microscopy (AFM) experiments are used in combination to predict and test which types of benzylic amide macrocycle-containing rotaxanes possess mobile components in the crystalline phase and thus could form the basis of solid-state devices that function through mechanical motion at the molecular level. The statistical studies and calculations show that crystals formed by rotaxanes possess similarities and unanticipated differences with respect to the crystal packing of noninterlocked molecules. Trends in the rotaxane series correlate quantities related to crystal packing, molecular size, stoichiometry, and H-bonding. In accordance with the findings of Gavezzotti et al. for conventional molecular architectures, a principal component analysis (PCA) showed that three vectors related to the size, packing parameters, and stoichiometry are sufficient to describe the crystal properties of benzylic amide macrocycle-containing rotaxanes. When hydrogen bond-related quantities are included in a second PCA, they combine with the size and the stoichiometry vectors but not with packing-related parameters, indicating that the intramolecular "saturation" of the H-bonds (between the interlocked components) takes precedence over crystal assembly (i.e., intermolecular packing) in these systems. However, cluster analyses also suggest a major role for the energy of interaction between the macrocycle and its crystal environment. The identification of such a "privileged" interaction is of fundamental importance to the development of rotaxanes with in-crystal mobility of one or more of their interlocked components, a prerequisite for the exploitation of molecular level mechanical motion in the solid state. The set of trends found, together with the calculated energies, was used to propose guidelines for which benzylic amide macrocycle-containing rotaxanes are best suited to become building blocks for systems with mobile submolecular units in the crystalline phase. An experimental test of the predictive power of such guidelines was carried out using AFM on a rotaxane and its thread, identified by the study as a promising candidate for solid-state mobility. Intuitively, the rotaxane should be less mobile in the solid state since it has multiple sets of both hydrogen bond donors and acceptors that can form strong inter- and intramolecular H-bonds. Conversely, the thread has no hydrogen bond donors and cannot form such bonds. The AFM experiments, however, confirm the statistical analysis prediction that the rotaxane is considerably more mobile in the solid than the thread.

Introduction

Molecules crystallize as the result of relatively weak interactions between the crystallizing components; noncovalent binding during the crystal assembly process ultimately yields a lower total energy than the individual components have with a solvent or at infinite distances. When considering molecules with mechanically interlocked molecular architectures, catenanes (interlocked rings) and rotaxanes (where a macrocycle is locked onto a linear thread by two bulky "stoppers"),[1] the picture is somewhat altered because the separation of the interlocked components is intrinsically restricted. The presence of a mechanical bond often enables the interlocked components to interact together in a very efficient manner, altering the mode of binding they could have on external species, in general, and

* To whom correspondence should be addressed. D.A.L.: E-mail, David.Leigh@ed.ac.uk. F.Z.: E-mail, gatto@ciam.unibo.it.
[†] Istituto di Spettroscopia Molecolare.
[‡] University of Warwick. Present address: Department of Chemistry, University of Edinburgh, The King's Buildings, West Mains Road, Edinburgh EH9 3JJ, U.K.
[§] Università degli Studi di Bologna.
[||] CLRC Daresbury Laboratory.

(1) (a) Amabilino, D. B.; Stoddart, J. F. *Chem. Rev.* **1995**, *95*, 2725−2828. (b) Sauvage, J.-P., Dietrich-Buchecker, C., Eds.; *Molecular Catenanes, Rotaxanes, and Knots*; Wiley-VCH: Weinheim, 1999.

10.1021/ja0159362 CCC: $22.00

within a crystal, in particular. The interlocking also generates special degrees of freedom where one submolecular unit may undergo large amplitude dynamics with respect to the other. The presence and the effects of these motions (including "shuttling" in the case of rotaxanes and "circumrotation" in the case of catenanes) are well-established in solution,[2] but only recently has it been seen in the solid,[3] the phase in which practical applications of such molecular architectures are likely to first find application. In fact, large amplitude intercomponent motions in catenane and rotaxane in the crystalline state are usually "locked" by intermolecular crystal packing interactions, and for such dynamics to exist on a reasonably fast, that is, millisecond-to-second time scale, the packing forces must necessarily be minimized. The forces bringing a molecular crystal together and the forces governing the ring dynamics are thus strongly connected, and their investigation can be carried out concomitantly. In the past, for molecules with conventional architectures, crystal structure analysis combined with molecular mechanics calculations proved that the cohesive, i.e., packing energy is interwoven with several molecular and crystal parameters (ranging from the number of valence electrons, to some packing indexes, to the molecular surface).[4] The approach pioneered by Gavezzotti was also able to ascertain that, out of a very large number of parameters one could consider, only the combination of size, packing, and stoichiometry parameters is necessary to describe the structural properties of a large number of organic crystals.[4] Here we apply this method to crystals of rotaxanes. The large family of rotaxanes based on a thread containing a hydrogen bonding template for the benzylic isophthalamide macrocycle, **1**,[5] offers a unique opportunity for investigating systematically the effect of intramolecular threading in the structures of crystals. It was the aim of this study to perform molecular mechanics calculations and structural analyses of the X-ray structures of benzylic amide rotaxanes to ascertain whether similarities or differences with other small organic molecules exist and to uncover a hierarchy of interactions and rules governing their crystal structures. The results provide a unique insight into which types of rotaxanes are more likely to show motion of the macrocycle in the solid state. The predictions were tested by carrying out atomic force microscopy (AFM) on a rotaxane and its corresponding thread, identified by the statistical analysis as a promising candidate for possessing mobility in the solid phase. Although the AFM tip does not probe directly the motion of submolecular units, an AFM experiment can provide indirect information on the packing interactions in the crystal. The AFM was used as a tool for scratching the crystal with a controlled load force. The load force, acting onto the surface of the (anisotropic) molecular crystal, modifies the material, as the shearing force exerted by the tip exceeds the adhesion forces within the crystal. The minimum load force required for scratching a comparable amount of material from a crystal is qualitatively related to the adhesion force, which depends on the packing interactions. Comparison of the miminum load forces for the rotaxane and its thread provides insight on the packing interactions in the solid state.

Computational Background

Recently, both the short time scale (subpicosecond), harmonic, and the long time scale (up to microsecond), large-amplitude, dynamics of benzylic amide macrocycle-containing catenanes and rotaxanes have been studied[6] using the MM3 model.[7] This force field was developed by fitting both heats of formation and structural results in the gas phase and in crystals of simple organics. MM3 is specifically parametrized to describe H-bonds in terms of dipole interactions and includes specific interatomic nonbonded potential energy functions that allow a quantitative treatment of the van der Waals and the electrostatic interactions which play an essential role in hydrogen bonding and in the $\pi-\pi$ interactions between aromatic rings. Despite the molecular complexities involved, the method successfully reproduces experimentally determined rotational barriers and steric energies in these types of catenane and rotaxane systems. All the calculations reported were performed using the TINKER package.[8] Ewald summation was used for the electrostatic interaction thereby including all the possible terms. The crystal structures of the rotaxanes were optimized starting from the structures determined by X-ray diffraction data. The reoptimization was necessary because the degree of disorder was not the same in all of the structures and was necessary to avoid

(2) See, for example: (a) Ballardini, R.; Balzani, V.; Credi, A.; Brown, C. L.; Gillard, R. E.; Montali, M.; Philp, D.; Stoddart, J. F.; Venturi, M.; White, A. J. P.; Williams, B. J.; Williams, D. J. *J. Am. Chem. Soc.* **1997**, *119*, 12503-12513. (b) Anelli, P.-L.; Spencer, N.; Stoddart, J. F. *J. Am. Chem. Soc.* **1991**, *113*, 5131−5133. (c) Ashton, P. R.; Bissell, R. A.; Spencer, N.; Stoddart, J. F.; Tolley, M. S. *Synlett* **1992**, 914−918. (d) Ashton, P. R.; Bissell, R. A.; Górski, R.; Philp, D.; Spencer, N.; Stoddart, J. F.; Tolley, M. S. *Synlett* **1992**, 919−922. (e) Ashton, P. R.; Bissell, R. A.; Spencer, N.; Stoddart, J. F.; Tolley, M. S. *Synlett* **1992**, 923−926. (f) Bissell, R. A.; Córdova, E.; Kaifer, A. E.; Stoddart, J. F. *Nature* **1994**, *369*, 133−137. (g) Benniston, A. C.; Harriman, A.; Lynch, V. M. *J. Am. Chem. Soc.* **1995**, *117*, 5275−5291. (h) Benniston, A. C. *Chem. Soc. Rev.* **1996**, *25*, 427−435. (i) Collin, J.-P.; Gavina, P.; Sauvage, J.-P. *Chem. Commun.* **1996**, 2005−2006. (j) Ashton, P. R.; Ballardini, R.; Balzani, V.; Boyd, S. E.; Credi, A.; Gandolfi, M. T.; Gómez-López, M.; Iqbal, S.; Philp, D.; Preece, J. A.; Prodi, L.; Ricketts, H. G.; Stoddart, J. F.; Tolley, M. S.; Venturi, M.; White, A. J. P.; Williams, D. J. *Chem.-Eur. J.* **1997**, *3*, 152−170. (k) Anelli, P.-L.; Asakawa, M.; Ashton, P. R.; Bissell, R. A.; Clavier, G.; Górski, R.; Kaifer, A. E.; Langford, S. J.; Mattersteig, G.; Menzer, S.; Philp, D.; Slawin, A. M. Z.; Spencer, N.; Stoddart, J. F.; Tolley, M. S.; Williams, D. J. *Chem.-Eur. J.* **1997**, *3*, 1113−1135. (l) Lane, A. S.; Leigh, D. A.; Murphy, A. *J. Am. Chem. Soc.* **1997**, *119*, 11092−11093. (m) Murakami, H.; Kawabuchi, A.; Kotoo, K.; Kunitake, M.; Nakashima, N. *J. Am. Chem. Soc.* **1997**, *119*, 7605−7606. (n) Gong, C.; Glass, T. E.; Gibson, H. W. *Macromolecules* **1998**, *31*, 308−313. (o) Leigh, D. A.; Troisi, A.; Zerbetto, F. *Angew. Chem., Int. Ed.* **2000**, *39*, 350−353. (p) Brouwer, A. M.; Frochot, C.; Gatti, F. G.; Leigh, D. A.; Mottier, L.; Paolucci, F.; Roffia, S.; Wurpel, G. W. H. *Science* **2001**, *291*, 2124−2128.

(3) (a) Cavallini, M.; Lazzaroni, R.; Zamboni, R.; Biscarini, F.; Timpel, D.; Zerbetto, F.; Clarkson, G. J.; Leigh, D. A. *J. Phys. Chem. B* **2001**, *105*, 10826−10830. (b) Gase, T.; Grando, D.; Chollet, P.-A.; Kajzar, F.; Murphy, A.; Leigh, D. A. *Adv. Mater.* **1999**, *11*, 1303−1306. (c) Collier, C. P.; Mattersteig, G.; Wong, E. W.; Beverly, K.; Sampaio, J.; Raymo, F. M.; Stoddart, J. F.; Heath, J. R. *Science* **2000**, *289*, 1172−1175.

(4) (a) Gavezzotti, A.; Desiraju, G. R. *Acta Crystallogr.* **1988**, *B44*, 427−434. (b) Gavezzotti, A. *J. Chem. Soc., Perkin Trans. 2* **1995**, 1399−1404. (c) Sorescu, D. C.; Rice, B. M.; Thompson, D. L. *J. Phys. Chem. A* **1999**, *103*, 989−998. (d) Gavezzotti, A. *J. Am. Chem. Soc.* **1989**, *111*, 1835−1843. (e) Gavezzotti, A. *J. Phys. Chem.* **1991**, *95*, 8948−8955. (f) Gavezzotti, A.; Filippini, G. *Acta Crystallogr.* **1992**, *B48*, 537−545. (g) Dunitz, J. D.; Gavezzotti, A. *Acc. Chem. Res.* **1999**, *32*, 677−684.

(5) (a) Johnston, A. G.; Leigh, D. A.; Murphy, A.; Smart, J. P.; Deegan, M. D. *J. Am. Chem. Soc.* **1996**, *118*, 10662−10663. (b) Leigh, D. A.; Murphy, A.; Smart, J. P.; Slawin, A. M. Z. *Angew. Chem., Int. Ed. Engl.* **1997**, *36*, 728−732. (c) Clegg, W.; Gimenez-Saiz, C.; Leigh, D. A.; Murphy, A.; Slawin, A. M. Z.; Teat, S. J. *J. Am. Chem. Soc.* **1999**, *121*, 4124−4129.

(6) (a) Leigh, D. A.; Murphy, A.; Smart, J. P.; Deleuze, M. S.; Zerbetto, F. *J. Am. Chem. Soc.* **1998**, *120*, 6458−6467. (b) Deleuze, M. S.; Leigh, D. A.; Zerbetto, F. *J. Am. Chem. Soc.* **1999**, *121*, 2364−2379. (c) Bermudez, V.; Capron, N.; Gase, T.; Gatti, F. G.; Kajzar, F.; Leigh, D. A.; Zerbetto, F.; Zhang, S. W. *Nature* **2000**, *406*, 608−611. (d) Fustin, C.-A.; Leigh, D. A.; Rudolf, P.; Timpel, D.; Zerbetto, F. *ChemPhysChem* **2000**, *1*, 97−100.

(7) (a) Allinger, N. L.; Yuh, Y. H.; Lii, J.-H. *J. Am. Chem. Soc.* **1989**, *23*, 8551−8566. (b) Lii, J.-H.; Allinger, N. L. *J. Am. Chem. Soc.* **1989**, *23*, 8566−8575. (c) Lii, J.-H.; Allinger, N. L. *J. Am. Chem. Soc.* **1989**, *23*, 8576−8582.

(8) (a) Ponder, J. W.; Richards, F. *J. Comput. Chem.* **1987**, *8*, 1016−1024. (b) Kundrot, C.; Ponder, J. W.; Richards, F. *J. Comput. Chem.* **1991**, *12*, 402−409. (c) Dudek, M. J.; Ponder, J. W. *J. Comput. Chem.* **1995**, *16*, 791−816.

Table 1. Comparison of the Packing Energies, Absolute Value in kcal mol^{-1}, of Selected Cases

system	CSD ref code	PE (lit)	PE (this work)
anthracene	ANTCEN	19.06[a]	20.01
ovalene	OVALEN01	38.47[a]	38.12
o-aminobenzoic acid	AMBACO03	24.19[b]	21.61
p-aminobenzoic acid	AMBNAC	25.67[b]	19.83
2,3-dimethyl-2,3-dinitrobutane	BECJEY	25.33[c]	22.21
2,2′,4,4′,6,6′-hexanitrostilbene	GIMBOT	51.67[c]	46.45
n-octane	OCTANE	14−17[d]	11.34
n-hexadecane		20−22[d]	19.35
tetrahydrofuran-3,4-dione	HYFURN	10−12[e]	8.43
(2*S*,3*S*)-tetrahydro-3-acetoxy-5-oxo-2,3-furan-dicarboxylic anhydride	CORZAK	14−18[e]	12.40
fumaronitrile	BISJIW	9−10[f]	10.94
phenanthridine	PHENAT	14−16[f]	17.48

[a] See ref 4a. [b] See ref 4b. [c] See ref 4c. [d] See ref 4d. [e] See ref 4e. [f] See ref 4f.

ambiguities caused by the definition of the position of the hydrogens (which are absent in X-ray structures). Comparison of the optimized structures with the X-ray structures showed only minor changes in the position of the heavy atoms.

For each of the minimized structures, the packing energy, PE, was calculated together with the molecular van der Waals surface, S_m, volume, V_m, and Kitaigorodski packing coefficient, C_k, that is, the ratio of the occupied to total volume of the cell. The atomic radii used to evaluate S_m, V_m, and C_k were taken from the work of Gavezzotti and co-workers on various organic systems.[4] To provide a firm comparison with previous work, a number of noninterlocked systems were treated with the same procedure. These examples were selected for their similarity with fragments of the rotaxanes studied here and can be described as fused ring aromatic hydrocarbons, disubstituted benzenes, nitro derivatives, hydrocarbons, oxohydrocarbons, and azahydrocarbons. On average, the discrepancy between previously reported values and the present ones is less than 10%, see Table 1.

Computational Results

Overall 28 crystal structures (**1**−**26**, Figure 1) were considered in the work, all of which are available in the Cambridge Crystallographic Database (the CCDC numbers are given in Table 2). The large majority of the molecules (25) were rotaxanes. Three extra cases were included to make the comparison more complete; the first was macrocycle **1** itself, the second was its interlocked dimer, the [2]catenane **2**, and the third was an example of a crystal structure of an uninterlocked thread **3**.

As a first step, we examined the solid-state structures to determine the correlation and interconnections that exist between various physical quantities. In this we mainly follow, with some additions, the well-established approach of Gavezzotti and coworkers.[4] The data also offered the opportunity to evaluate which rotaxanes may show "crystal plasticity" (i.e., retaining the order induced through intermolecular packing, but distorting the original structure through mechanical perturbations) and/or mobility of the macrocycle in the solid phase. Both these properties can appear if some of the noncovalent bonding interactions in the crystal are energetically low. In the first case, plasticity can arise as a result of low packing energies; in the second case, ring mobility may be caused if the ring−thread and the ring−external environment interactions are both low. In both cases, a low density of the solid would assist the phenomena. These two properties are of particular interest because applications of rotaxanes and catenanes in materials science applications and/or molecular level devices are both likely to depend on inducing movements in the interlocked components in the solid state. For example, a rotaxane displaying a high degree of plasticity could be used for surface patterning with an AFM tip, while the ring mobility (e.g., shuttling) could be exploited to create solid-state devices based on the variation of other properties (e.g., fluorescence) triggered by purely mechanical motion.

Initially, the simplest approach is to focus on the energy trends, some of which emerge clearly. Table 2 shows a summary of the molecular mechanics energies. The packing energies, PE, range from 51.1 to 93.0 kcal mol^{-1}. Each PE contains three contributions, that is, H-bonding, $\pi-\pi$ stacking, and other van der Waals interactions. In quantitative terms, each one plays a similar role, with the $\pi-\pi$ stacking interactions usually giving the largest contribution. No direct correlation was found between PE and H-bonding and $\pi-\pi$ stacking energies, while a fair correlation, $r = 0.67$, was obtained by fitting PE versus the energy of other van der Waals interactions. Somewhat surprisingly, the lack of a direct correlation between H-bond energy or $\pi-\pi$ stack energy and PE indicates that there is no common mode of interaction which dominates the way these rotaxanes interact within their crystals. In other words, the visual inspection of the data shows that the stoppers, which can usually create $\pi-\pi$ stacking interactions, and the isophthalamide macrocycle, which can create both H-bonding and $\pi-\pi$ stacking interactions, contribute to hold together the crystals using noncorrelated amounts of the three different kinds of noncovalent forces.

Attention was then given to the interactions of one of the two mechanically connected units, the macrocycle, either with the thread or within the crystal lattice. A good correlation, $r = 0.87$, was obtained by fitting the PE versus the interaction energy of the macrocycle with its crystal environment. The proportionality is important because it reduces the complexity of the considerations one has to make to understand the forces that exist in the rotaxane solid-state structures. Interestingly, the proportionality holds for each of the three energy components mentioned above when the rotaxane−crystal and the macrocycle−environment energies are considered. The correlation coefficients were (i) for the hydrogen bond energy, $r = 0.95$, (ii) for the $\pi-\pi$ stacking energy, $r = 0.82$, and (iii) for the other van der Waals energy contributions, $r = 0.92$. Other fittings of the various types of energy were attempted without success. *The analysis of the molecular mechanics calculations shows that each component of the packing energy tends to scale with the same component of the energy of interaction between the macrocycle and its crystal environment.*

To establish the effects of mechanical interlocking, the calculated energies must also be compared with those of other types of molecules (Figure 2). Figure 2a shows that this class of rotaxanes, for low packing coefficients, tends to pack with a packing energy intermediate between those of low molecular weight organic compounds and proteins.[9] Qualitatively, it is the presence of multiple hydrogen bonds that makes loose packing

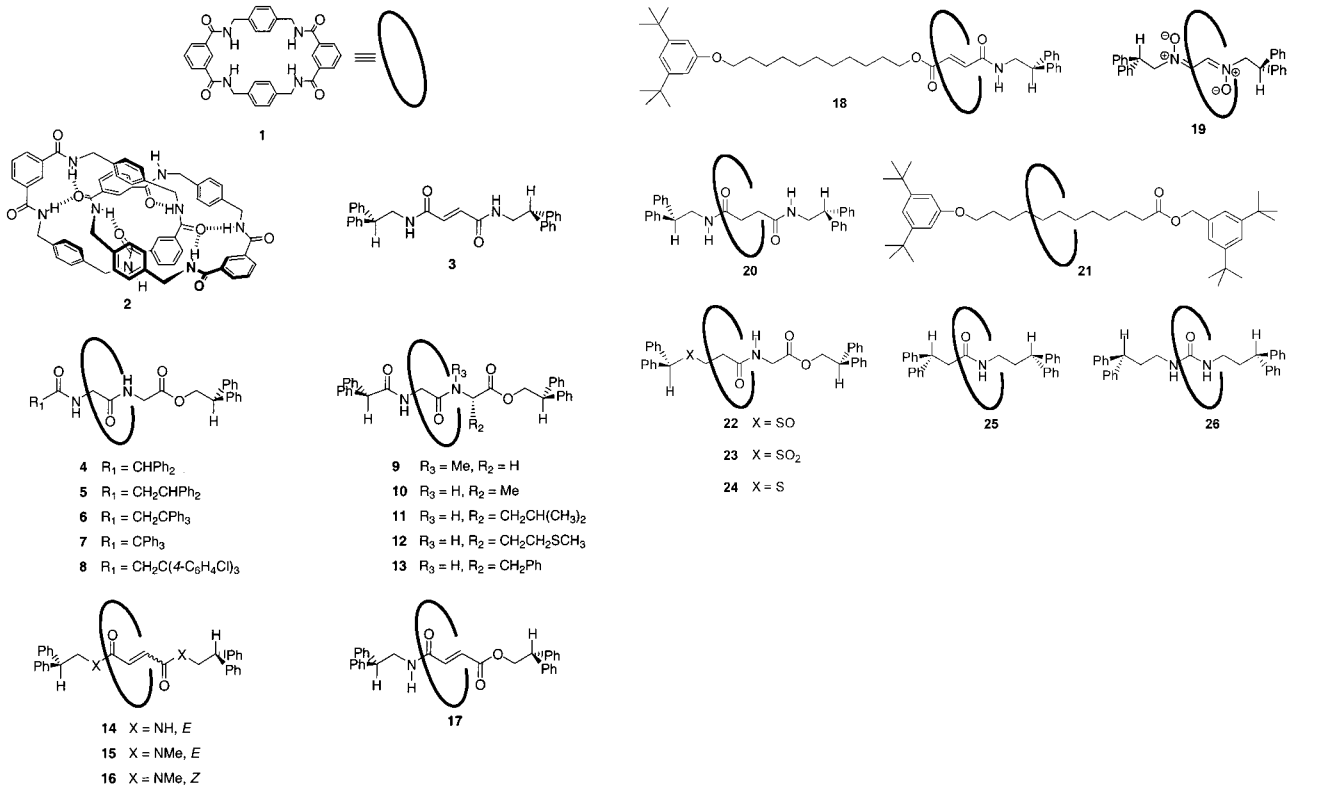

Figure 1. Molecules **1**−**26** investigated in this work.

Table 2. Noncovalent Inter- and Intramolecular Energy Contributions, Absolute Value in kcal mol^{-1}, for the Crystal Structures[a]

	molecule–crystal				macrocycle–thread[b]				macrocycle–crystal				
system	HB	$\pi\pi$	vdW	PE	HB	$\pi\pi$	vdW	tot	HB	$\pi\pi$	vdW	tot	CCCD
1	29.7	8.5	12.5	50.7									157 384
2	19.9	13.5	20.5	53.9	25.4	8.1	19.3	52.8	9.9	6.8	10.3	27.0	160 504
3	16.0	10.6	22.0	48.6									160 651
4	11.6	33.4	18.8	63.8	14.7	7.7	12.6	35.0	9.0	17.7	7.4	34.1	101 367
5	20.5	39.6	14.8	74.9	14.6	6.9	10.6	32.2	14.4	18.5	8.4	41.3	161 350
6	1.9	37.6	25.6	65.1	17.8	10.6	16.9	45.3	1.2	17.4	15.4	34.0	161 351
7	12.1	35.7	13.6	61.4	14.4	9.8	12.7	36.9	10.1	16.4	6.7	33.2	161 352
8	19.0	41.9	31.3	92.2	15.2	8.8	12.5	36.5	14.6	18.0	10.2	42.8	160 505
9	5.8	35.8	16.8	58.3	13.6	11.0	15.5	40.1	5.8	19.1	8.1	33.0	179−101 321
10	3.1	33.2	19.5	55.8	18.8	8.1	16.5	43.4	1.5	17.3	11.0	29.8	147 201
11	0.0	34.5	26.0	60.5	18.9	9.6	19.1	47.6	0.0	18.4	14.5	32.9	101 368
12	16.1	31.5	31.3	77.0	13.9	10.0	13.6	37.6	9.4	16.5	12.4	38.3	101 369
13	11.5	34.1	47.4	93.0	18.7	10.8	17.0	46.5	3.7	17.8	29.1	50.6	101 370
***14a*[c]**	*0.0*	*30.6*	*25.7*	*56.3*	*23.5*	*8.3*	*21.7*	*53.5*	*0.0*	*18.1*	*19.4*	*37.5*	157 383
(DMSO)	7.1	30.6	32.9	70.6	16.4	8.3	12.8	37.5	0.0	18.1	22.6	40.7	
***14b*[c]**	*0.0*	*43.7*	*19.4*	*63.1*	*27.4*	*7.4*	*31.6*	*66.4*	*0.0*	*23.2*	*6.2*	*29.4*	140 045
(DMF)	4.7	43.7	43.0	91.4	18.1	7.4	12.3	37.8	0.0	23.2	12.6	*35.8*	
14c (acetonitrile)	24.0	36.2	43.0	79.0	9.2	7.9	9.4	26.4	17.0	16.7	14.0	47.7	160 650
15	0.0	32.7	22.3	55.0	19.1	10.8	18.0	47.9	0.0	14.1	15.5	29.6	149 673
16	8.7	36.7	13.4	58.8	9.8	11.0	19.8	40.6	8.7	17.2	5.7	31.6	149 672
17	19.5	28.8	21.8	70.1	9.6	8.0	9.0	26.6	16.9	15.3	7.8	40.0	140 046
18	6.1	33.7	29.2	69.0	10.7	8.5	11.7	30.9	4.5	21.2	18.5	44.2	160 506
19	11.1	36.4	4.5	51.1	4.8	9.1	15.3	29.1	11.1	16.5	3.4	31.0	146 020
20	29.1	22.6	20.2	71.8	7.5	6.7	9.7	23.9	22.6	11.5	9.3	43.4	157 381
21	7.8	12.7	58.0	78.4	9.7	5.1	15.8	30.6	7.8	9.6	33.6	51.0	127 612
22	8.0	29.6	18.3	55.8	24.4	9.5	12.0	46.0	5.0	14.8	10.7	30.5	161 353
23	7.8	26.7	39.5	74.0	21.7	11.5	15.9	49.2	7.8	13.5	19.8	41.1	160 507
24	6.5	32.8	17.5	56.8	15.1	7.2	16.7	39.0	6.5	17.7	8.1	32.3	160 649
25	12.4	33.0	12.8	58.1	8.9	9.1	21.5	39.5	12.4	14.3	8.5	35.2	160 648
26	28.7	27.4	34.3	90.4	9.4	9.4	17.0	35.8	17.5	11.8	19.3	48.6	157 380

[a] HB indicates the energy of hydrogen-bonding; $\pi\pi$ indicates the energy of the π-electron stacks; vdW indicates the energy of the remaining van der Waals contributions; PE is the packing energy. [b] For isophthalamide catenane **2**, these terms correspond to the macrocycle−macrocycle intramolecular interactions. [c] For these rotaxanes, the first row (in *italics*) gives the values for the "complex" formed by one rotaxane molecule and its nearest solvent molecules, while the values in the second row refer to the rotaxane molecule alone. Both were included in the Supporting Information.

energetically very efficient. Significantly, the macrocycle, **1**, its interlocked dimer, **2**, and the thread, **3**, fall inside the bracket typical of low molecular weight organic compounds. The apparent difference between rotaxanes and the other small

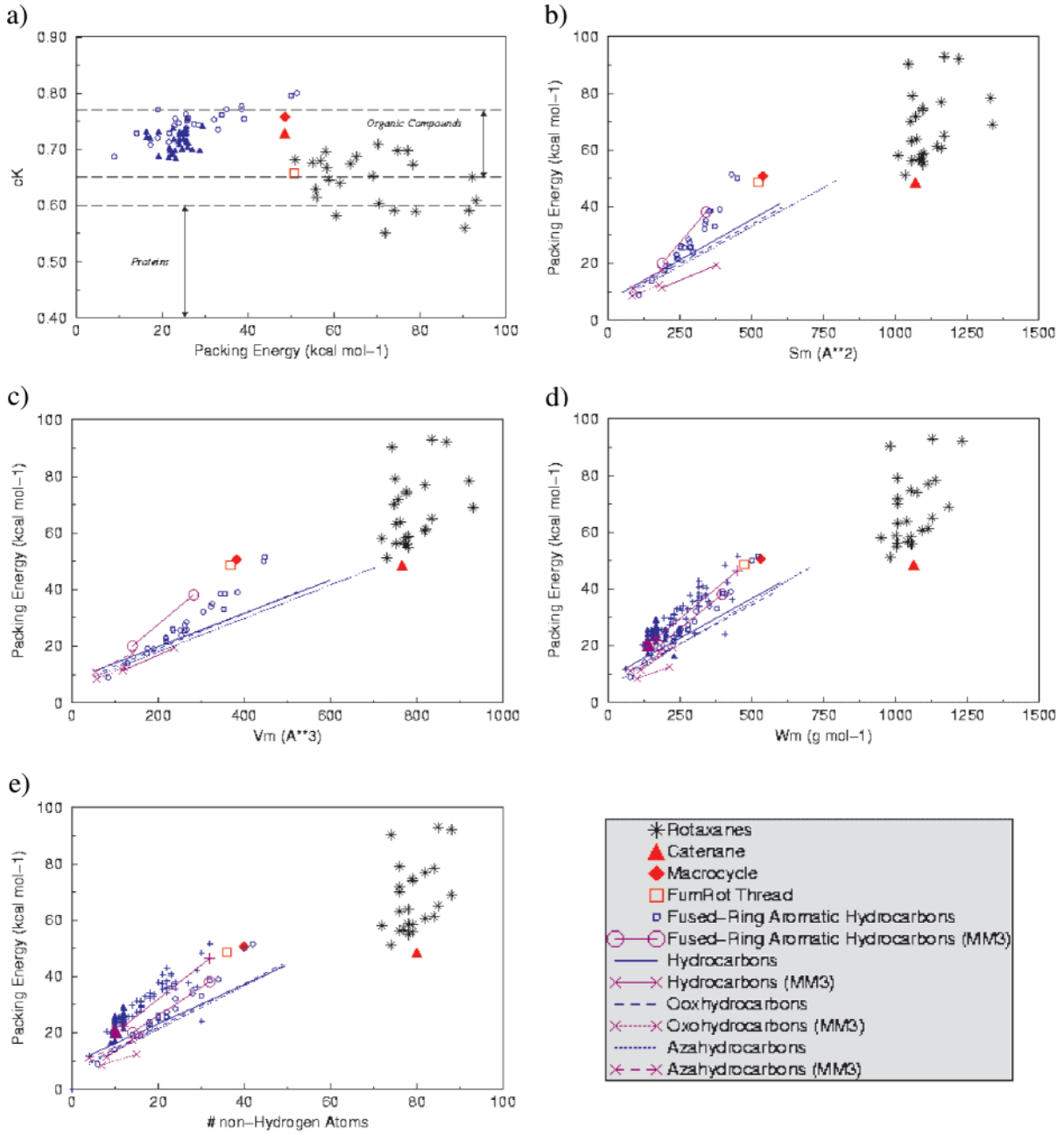

Figure 2. (a) Comparison of packing coefficients versus packing energies; (b) packing energies versus molecular surfaces; (c) packing energies versus molecular volumes; (d) packing energies versus molecular weights; (e) packing energies versus the number of nonhydrogen atoms.

organic molecules of Figure 2a ceases to exist when one considers Figure 2b−e, where packing energies are plotted versus molecular surfaces, volumes, weights, and the number of nonhydrogen atoms. Extrapolation of the data for organic molecules smaller than the rotaxanes shows that their data are located within the ideal bracket area generated by typical organic molecules. *Comparison with other small organic molecules therefore emphasizes a prominent role in the packing of intermolecular hydrogen bonding, but proves that many properties of benzylic amide macrocycle-containing rotaxanes tend to have similar trends to those of noninterlocked molecules.*

More quantitative correlations between the molecular mechanics results and the molecular parameters can be attempted following previous work[4] with the principal component analysis (PCA). As in the case of the extensive work carried out by Gavezzotti and co-workers,[4] the properties were divided into (i) size parameters, (ii) stoichiometry parameters, and (iii) packing parameters. The size parameters were W_m, the molecular weight, Z_v, the number of valence electrons, S_m, the molecular surface, V_m, the molecular volume, PE, the packing energy, and N_{nonH}, the number of nonhydrogen atoms.

The stoichiometry parameters were N_{nonH}/N_H, the ratio of the number of nonhydrogen atoms over the number of hydrogen atoms, S_{nonH}/S_H, the ratio of the surface of the nonhydrogen

(9) For organic compounds the Kitaigorodski index range is 0.65−0.77, see: (a) Kitaigorodski, A. I. *Molecular Crystals and Molecules*; Academic Press: New York, 1973; p 167. For proteins the Kitaigorodski index range is 0.40−0.60, see: (b) Crick, F. H. C.; Kendrew, J. C. *J. Mol. Biol.* **1968**, *33*, 491−497. (c) Andersson, K. M.; Hormöller, S. *Acta Crystallogr.* **2000**, *D56*, 789−790.

Table 3. Composition of the Factors in the Principal Component Analysis[a]

Eigenvalues	1	2	3	4	5
value	6.312	5.927	3.307	2.427	0.805
% of variability	32	30	17	12	4
cumulative %	32	61	78	90	94

Vectors	1	2	3	4	5
PE	0.15	0.27	−0.16	0.29	−0.25
E_{mac-th}	−0.24	−0.21	−0.27		
E_{mac-xt}	0.16	0.31	−0.12		−0.38
E_{hb}	0.27		−0.23	0.31	
$E_{hb(intra)}$	−0.23	−0.16	−0.30	0.21	
$E_{hb(inter)}$	0.36	0.14		0.11	
$E_{hb(mac)}$	0.36	0.11	0.10		0.14
$r_{hb(1)}$	0.35	0.16			
$r_{hb(2)}$	0.35	0.15	0.10		0.11
W_m	−0.19	0.29		0.31	0.10
Z_v	−0.23	0.32		0.12	
S_m	−0.21	0.35			
V_m	−0.21	0.35			
N_{nonH}	−0.22	0.29		0.27	0.10
N_{nonH}/N_H	0.10	−0.24		0.43	0.32
S_{nonH}/S_H		−0.22	−0.12	0.47	
V_m/S_m		0.23		−0.11	0.77
D_c		−0.10	0.45	0.32	
D_{el}		−0.10	0.49	0.17	
C_k			0.51	0.11	

[a] Coefficients <0.1 in absolute values have been omitted.

atoms over the surface of the hydrogen atoms, and V_m/S_m, the exposure ratio.

The packing parameters were D_c, the density, D_{el}, the number of electrons per unit volume in the cell, and C_k, the Kitaigorodski packing coefficient.

Only the bulk modulus at zero pressure and 60% of the melting temperature was not included in the analysis since these values are not available for these molecules. As in the case of hydrocarbons,[4g] the multidimensional space is reduced by PCA to a three-dimensional space. The first component is dominated by the size parameters, while the other two are best described as in-phase and out-of-phase combinations of packing and stoichiometry parameters. This further indicates that, in many senses, the crystal properties of interlocked systems do not differ from those of the standard systems. The presence of threading, however, creates a large number of hydrogen bonds that can be taken as its mark. A second PCA was then carried out with eight new parameters: E_{mac-th}, the interaction energy macrocycle−thread, E_{mac-xt}, the interaction energy of the macrocycle with the rest of its environment, E_{hb}, the total hydrogen bonding energy, $E_{hb(intra)}$, the hydrogen bonding energy for the interaction between the macrocycle and the thread, $E_{hb(inter)}$, the intermolecular hydrogen bonding energy, $E_{hb(mac)}$, the intermolecular hydrogen bonding energy of the macrocycle, $r_{hb(1)} = N_{hb(inter)}/N_{hb(intra)}$, the ratio of the inter- and intramolecular hydrogen bonds, and $r_{hb(2)} = N_{hb(mac)}/N_{hb(intra)}$, the ratio of the inter- and intramolecular hydrogen bonds of the macrocycle.

The various types of energy strongly correlate with each other as all the hydrogen-bond-related quantities do. The nearly block matrix of the hydrocarbons[4] for the size, stoichiometry, and packing components is preserved. Table 3 shows the composition of the PCA matrix eigenvectors. The 20-dimensional space of the parameters reduces to a 5-dimensional space with only 6% loss of information. This is similar to that found by Dunitz and Gavezzotti for hydrocarbons.[4g] The 20 quantities are so strongly interdependent that only a combination of five of them suffices to describe all the others. The first two descriptors, that is, eigenvectors, are the plus and minus combinations of the previously found size-related eigenvector with the hydrogen bond parameters. *The description of size and H-bonds is therefore intrinsically entangled*. The third eigenvector is similar to the packing terms dominated vector found for the hydrocarbons. The last two eigenvectors are the plus and minus combinations of the previously found stoichiometry-related eigenvector with hydrogen bond parameters. *The description of stoichiometry and H-bonding is therefore also intrinsically entangled*. The entanglement arises on a statistical basis and may have different individual origins; for instance, in the series from 4 to 13 the structural variations do not modify the H-bonding groups but change either a stopper or a side chain of the thread. Increasing the size of a stopper decreases the intermolecular H-bond capability (and therefore increases the intramolecular one), while increasing the size of a side chain in the thread disrupts the possibility of intramolecular hydrogen bonds (and therefore increases the possibility of intermolecular bonding).

The preferential mixing of hydrogen bond quantities with the size and the stoichiometry parameters and the lack of an equivalent mixing with the packing parameters suggest that packing properties are not determined by H-bonding. This is a surprising result in view of the low crystal density of this class of rotaxanes which is readily ascribed to the presence of multiple hydrogen bonds. *The straightforward interpretation one can offer is that intramolecular "saturation" of the H-bonds takes precedence over their use in the crystal assembly. In terms of a hypothetical hierarchy of phenomena, the establishment of H-bonds intramolecularly is physically of higher importance than the actual crystal density*, a feature that one might attempt to exploit for crystal engineering.

The principal component analysis gives a picture similar to that obtained for other organic systems with the additional inference offered for the different roles of intra- and intermolecular H-bonds. While it is highly satisfactory that only a few components suffice to describe the packing of these materials, the strong interconnection shown by the various parameters fails in providing a simple understanding of the "rules of the game" for the crystal structures of these compounds. Accordingly, cluster analysis (CA) was then used to determine the existence of partial correlation between subsets of rotaxanes, where the PE scales with one or more of the quantities were used in the PCA. The clusters were formed for five different properties, Table 4: (i) the intermolecular hydrogen bond strength, which, pursuing the analogy with proteins, is responsible for the low crystal density; (2) the strength of interaction between the macrocycle and the thread, from which partly depends the possibility of motion of the macrocycle; (3) the strength of interaction between the macrocycle and the environment, which is the second energy component from which depends the possibility of motion of the macrocycle; (4) the crystal density, whose low value would provide an environment for motion of the macrocycle; and (5) the Kitaigorodski packing coefficient, which also has to be low for motion of the macrocycle to exist.

The exact ranges of values that bracket the clusters are shown for each of the five properties listed above in column 4 of Table 4. In many cases, it was possible to obtain a further correlation

Table 4. Cluster Analysis: The Rotaxanes Are Divided into Five Sets of Several Clusters of Differing Ranges of One of the Parameters Studied[a]

$E_{hb(inter)}$	cluster	rotaxanes	property	slope	intercept	r
0−3.1	1	6, 10, 11, 14a, 14b, 15				
5.8−16.1	2	4, 7, 9, 12, 13, 16, 18, 19, 21, 22, 23, 24, 25	E_{mac-xt}	0.55	1.35	0.90
19−29.1	3	5, 8, 14c, 17, 20, 26	E_{mac-th}	1.52	33.78	0.86
			$E_{\pi-\pi(intra)}$	7.39	20.98	0.82
E_{mac-th}						
23.9−32.2	1	5, 14c, 17, 18, 19, 20, 21	E_{mac-xt}	0.62	−0.77	0.91
35.0−40.1	2	4, 7, 8, 9, 12, 24, 25, 26	E_{mac-xt}	2.28	−18.42	0.94
43.4−66.4	3	6, 10, 11, 13, 14a, 14b, 15, 16, 22, 23	E_{mac-xt}	1.59	8.46	0.91
E_{mac-xt}						
29.4−35.2	1	4, 6, 7, 9, 10, 11, 14b, 15, 16, 19, 22, 24, 25				
37.5−44.2	2	5, 8, 12, 14a, 17, 18, 20, 24				
47.7−51.0	3	13, 14c, 21, 26	E_{mac-th}	1.03	−52.62	0.90
D_c						
1.06−1.14	1	10, 13, 14a−c, 16, 18, 21, 22, 23	E_{mac-xt}	1.28	17.90	0.89
1.17−1.30	2	4, 5, 6, 7, 8, 9, 12, 15, 17, 19, 25, 26	E_{mac-xt}	2.50	−23.04	0.91
			W_m	0.11	−55.99	0.76
C_k						
0.58−0.61	1	11, 13, 14a−c, 22, 23	E_{mac-xt}	1.47	11.99	0.89
0.63−0.65	2	7, 8, 10, 16, 18	E_{mac-xt}	1.74	4.12	0.81
			$r_{hb(1)}$	22.53	33.25	0.84
			W_m	0.15	−96.95	0.89
			N_{nonH}	2.59	−148.99	0.81
0.67−0.71	3	4, 5, 6, 9, 12, 15, 17, 19, 21, 24, 25	E_{mac-xt}	1.34	15.77	0.86

[a] The nature and ranges for the parameter are given in column 1. In column 4, the property that correlates with the packing energy is given, and, in column 7, the results of the linear regression are given.

within the cluster between the packing energy and the properties shown in column 4. For instance, in the first set of entries in the table, the rotaxanes divide into three clusters of increasing intermolecular hydrogen bonding strength. For medium H-bond strengths (5.8−16.1 kcal mol^{-1}), the packing energy scales with the energy of interaction between the macrocycle and its crystal environment. This correlation had already been observed for the whole series; however, in this cluster, the value of r increases from 0.87 to 0.90. For large H-bond strengths, the packing energy correlates both with the energy of interaction of the macrocycle with the thread and with the $\pi-\pi$ stacking energy. Where strong H-bonds can be formed, it is the interactions of the macrocycle that govern the packing energy.

In the second set of entries of Table 4, three clusters form with respect to the energy of interaction between the macrocycle and the thread. Within each cluster there is a further correlation between the packing energy of the rotaxane and the energy of interaction of the macrocycle and its external environment. This indicates that these types of energies (E_{mac-th} and E_{mac-xt}) are strongly related as one would, perhaps, expect.

In the third entry, clusters are also formed as a function of the interaction between the macrocycle and its external environment. Only when such an interaction is large, the packing energy correlates with the strength of the macrocycle−thread interaction.

The density and the Kitaigorodski packing coefficient (last two entries) also form clusters where there is further correlation between the packing energy and a number of other parameters. The already fair general correlation obtained for packing energy versus the macrocycle−crystal environment interactions, $r = 0.87$, tends to improve within each cluster.

The cluster analysis shows that, regardless of the parameter considered, a prominent role is played in the packing energy by the interactions between the macrocycle and its crystal environment.

The existence of general trends within this large family of rotaxanes is rewarding. The question, however, arises whether one can make predictions on a specific rotaxane using the knowledge of these data. The unusual degree of freedom that exists in these systems offers the opportunity of *ad hoc* investigations. To create mobility of the ring in the solid or on a surface, one requires weak inter- and intramolecular interactions and the possibility of "maneuvering" which, in general, is provided by shape compatibility. Since all the molecules studied here have rather similar shapes, other parameters such as density must be considered. The ring mobility can be instrumental for crystal plasticity which can be obtained partly through the rings motion. It can also be used *per se* to give switchable polymorphic phases. Figure 3 shows 3-D plots of (a) density versus packing energy versus the sum of the interaction energy of the macrocycle−thread and macrocycle−crystal environment and (b) density versus interaction energy of the macrocycle−thread versus the interaction energy of the macrocycle−crystal environment. A "compromise" for a low value of the three quantities exists; rotaxanes **14** (crystallized from DMSO and DMF), **15**, **16**, **18**, **20**, and **22** are the best suited. Their threads are based on fumaramide, succinamide, and various sulfur-based motifs. The fumaramide-based rotaxanes **14** and **15** are particularly interesting in this respect, since they can be prepared in high yields[6c] and are now being explored by AFM techniques to verify their potential.

Testing the Prediction

The analysis of the calculations has focused on a few types of rotaxanes that should be characterized by high solid-state mobility. We checked the existence of such high mobility by AFM for a candidate rotaxane **15**, which appeared promising from the statistical studies, and compared it to its thread. In fact, *a priori* this system intuitively appears unlikely to possess increased mobility in the rotaxane because the thread has no hydrogen bond donors and thus cannot form strong intermolecular hydrogen bonds in the solid state by itself, whereas the rotaxane has multiple sets of both hydrogen bond donors and

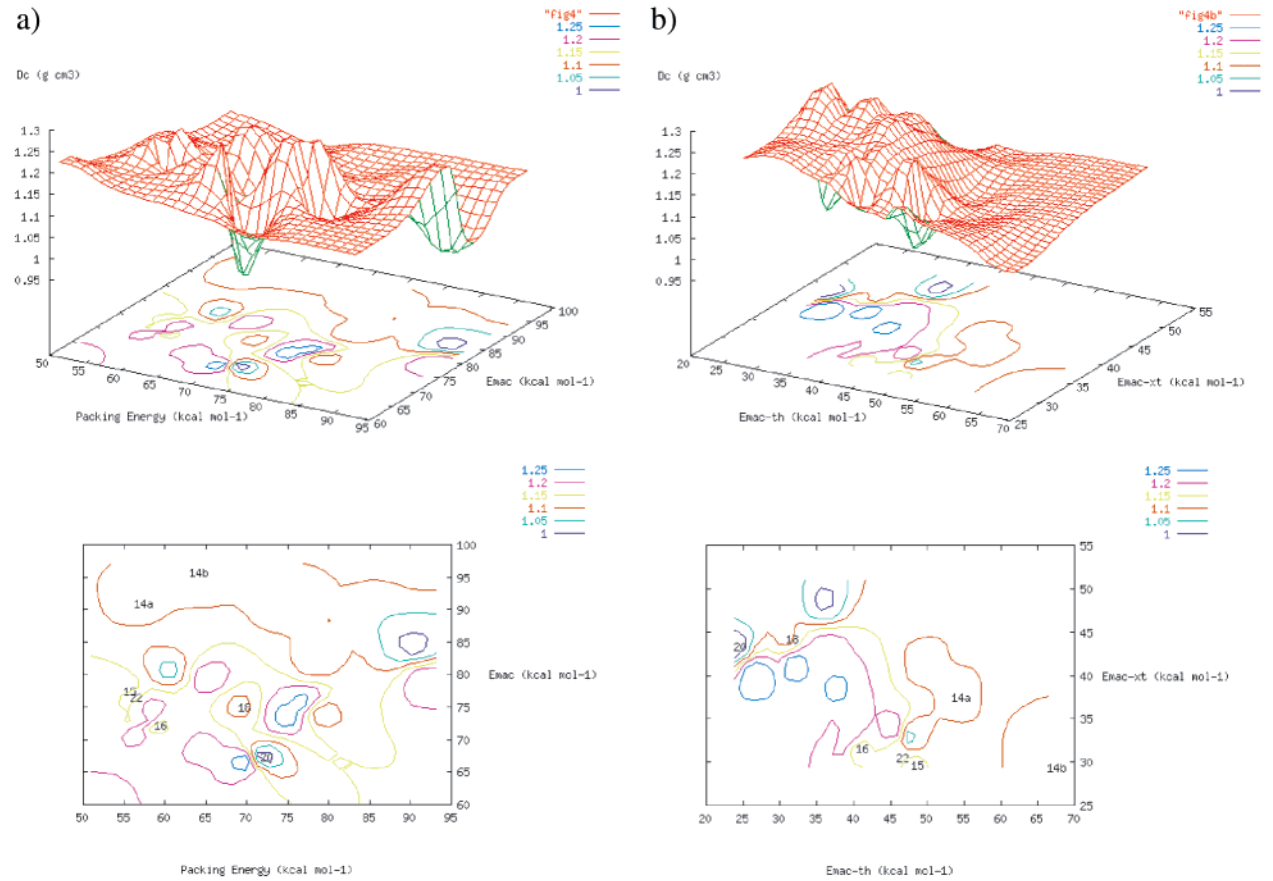

Figure 3. (a) Density versus packing energy versus the sum of the interaction energy of the macrocycle−thread and macrocycle−crystal environment; (b) density versus interaction energy of the macrocycle−thread versus the interaction energy of the macrocycle−crystal environment.

acceptors which can form both strong and directional inter- and intramolecular H-bonds.

Figure 4 shows the morphology of a crystal of rotaxane **15** with terraces and well-defined angles (90°) which indicates growth oriented on the *ab* plane of the monoclinic crystal. The line profile (see Figure 4b) shows terrace steps which are integer multiples of 1.0 ± 0.1 nm. This distance matches the lattice distance along the *c* axis. The typical force used for imaging the crystals in contact mode ranged between 0.5 and 0.8 nN. Figure 4c and d shows the result of scanning a 500 nm by 500 nm area of the crystal surface by increasing the load force from 0.5 to 2 nN. The higher force modifies the top two layers within the scanned area. Friction force microscopy reveals a strong contrast of the modified area with respect to the rest of the crystal. The root-mean-square roughness of the surface increases from 0.704 nm outside to 1.32 nm inside the scratched area.

We repeated the experiment using the same cantilever on the crystal of the thread of **15** and adopting the same experimental conditions (i.e., scan rate, duration of the maximum load force). The unchanged quality of the tip was checked by acquiring topography of the thread crystal. To obtain the same result, an increase in the load force from 0.5 to 14 nN is required. This is nearly one order of magnitude higher than in the rotaxane.

This result confirms the theoretical prediction that interlocking with the macrocycle leads to higher mobility of **15** in the solid state**.** Although this mobility may be associated with either intra- or intermolecular movement, the statistical treatment of rotaxane crystal structures can clearly be used to predict which type of rotaxane building blocks may show mechanical movement in the solid state.

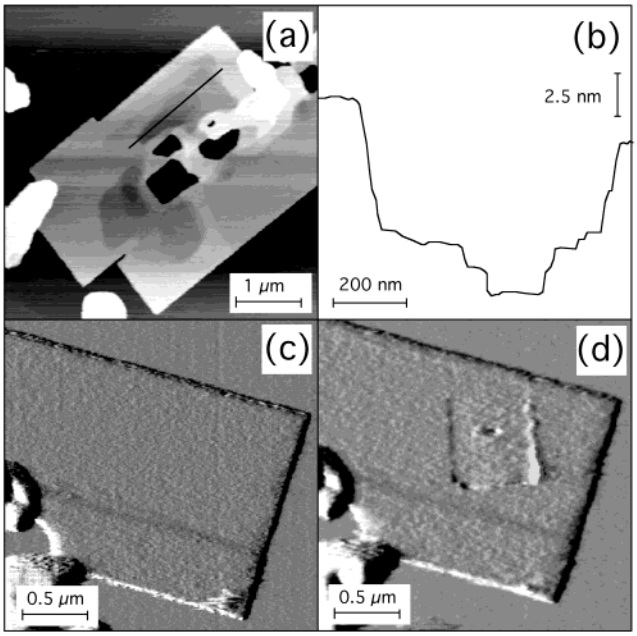

Figure 4. (a) AFM topographical image (height range $z = 0-45$ nm) of rotaxane **15** microcrystals obtained by deposition from an acetone solution followed by annealing for 7 min in air at 420 K. Set point load force is 0.5 N. (b) Profile along the solid line shown in (a); the terraces have a step height ∼1.0 ± 0.1 nm. (c) AFM image (error signal) before and after (d) surface patterning with a 2 nN load force.

Some Rules and Conclusions

This paper is ultimately about the comparative ability of macrocycle **1** to bind to other molecules inside and outside its cavity. The conclusions one can gather, which are ultimately important for the future design of benzylic amide macrocycle-containing rotaxanes that can shuttle and/or spin in the solid state, can be put in the form of some simple rules of thumb: (1) Comparison of the rotaxane crystal structures with other small organic molecules and proteins shows a prominent role of the hydrogen bond in rotaxane packing. (2) Analysis of molecular mechanics calculations shows that each of the three energy components of the packing energy (H-bond, $\pi-\pi$ stack, and other van der Waals) of the rotaxanes tends to scale with the same component of the energy of interaction between the macrocycle and its crystal environment. (3) The PCA showed that many properties of the crystal structures of benzylic amide macrocycle-containing rotaxanes tend to have trends similar to those of noninterlocked small organic molecules. (4) The PCA showed that the description of molecular size and H-bonds is strongly interrelated. (5) The PCA showed that the description of stoichiometry and H-bonds is strongly interrelated. (6) Formation of intramolecular hydrogen bonds in these carefully designed rotaxane systems often takes precedence over their use in the crystal assembly. Therefore, establishing intramolecular interactions is of higher importance than the crystal density. (7) The cluster analysis shows that, regardless of the parameter considered, a very prominent role is played in the packing energy by the interactions between the macrocycle and its crystal environment.

Apart from this set of simple rules, the present work further shows that the key properties of low crystal packing density and weak macrocycle interactions can co-exist and that by using the computational protocol partly developed here it is possible to select a rotaxane where the presence of the macrocycle induces a higher mobility in the solid. AFM experiments corroborated the predictions made for one of the rotaxanes, showing that this system presents higher in-crystal mobility than its thread. Such results are important for the selection of rotaxane building blocks that could act as components for molecular shuttles and machines which would function as part of a solid-state device.

Atomic Force Microscopy Experimental Procedure

Films of both a promising candidate rotaxane (**15**) and its corresponding thread were grown by drop-casting from acetone (Aldrich, chromatography grade) solutions (0.4 mg/mL) onto highly oriented phyrolitic graphite (HOPG) which was cleaved prior to drop casting. To obtain molecular crystals, both rotaxane and thread films were annealed for 7 min in air at 100−120 °C. Both compounds form tiny crystals with the shape of the rotaxane crystals being better defined. An atomic force microscope operated in contact mode was used both for imaging and for performing lithography with silicon oxide tips (Ultralevers, Thermomicroscope, USA) with 10 nm nominal radius of curvature and cantilevers with a force constant equal to 0.24 N/m (min 0.10−max 0.47 N/m).

Acknowledgment. We would like to thank the referees for encouraging us to experimentally check the prediction of higher solid-state mobility for the fumaramide rotaxanes and Ricardo García for useful discussions. This work was partly supported by the TMR initiative of the European Union through contracts FMRX-CT96-0059 and FMRX-CT97-0097. F.Z. also acknowledges partial support from MURST project "Dispositivi Supramolecolari" and the University of Bologna "Funds for selected research topics" initiative. D.A.L. is an EPSRC Advanced Research Fellow (AF/982324).

Supporting Information Available: A table with the PCA correlations matrix, plots of the correlation between some noncovalent interactions (PDF). This material is available free of charge via the Internet at http://pubs.acs.org.

JA0159362